Assessment of residual stresses and mechanical characterization of materials by "hole drilling" and indentation tests combined and by inverse analysis

V. Buljak [a], G. Cocchetti [b], A. Cornaggia [b], G. Maier [b,*]

[a] *Department of Strength of Materials, Faculty of Mechanical Engineering, University of Belgrade, Kraljice Marije 16, Belgrade, Serbia*
[b] *Department of Civil and Environmental Engineering, Politecnico di Milano (Technical University), Piazza Leonardo da Vinci 32, 20133, Milan, Italy*

Received 28 January 2015
Accepted 17 February 2015
Available online 7 March 2015

Dedicated to the 90th anniversary of
Professor Bruno Boley.

1. Introduction

Residual stresses generated by manufacture or service may be a major factor causing failures of structural components in a variety of engineering context. The assessments at the macro-scale of residual stresses, and of stresses generated by deteriorating events, are at present often performed by the "semi-destructive" Hole Drilling (HD) method. This method is described with details, standardized and compared to alternative techniques in a vast recent literature (see e.g. [1–6]).

Also instrumented indentation (IND) (historically originated from "hardness tests" on structural metals) is widely dealt with in present literature, where some specific issues related to this study are elaborated and discussed [7–10].

In the present paper, a sequential combination of HD test and instrumented indentation (mentioned here henceforth by HD + IND) is proposed for structural diagnosis, with a central methodological role played by "inverse analyses".

The operative procedure with some details on the main novel features is outlined in Section 2.

Section 3 specifies the residual stress modelling considered and its parameters to identify, the selected mechanical model of metallic materials and the finite element simulations of the test. Test simulations ("direct analyses") and assessments of "sensitivities" linking measurable quantities to sought parameters are presented in Section 4.

Section 5 synthesizes the deterministic method adopted herein for "inverse analyses" as mathematically supported transitions from experimental data to the sought estimates of selected mechanical quantities ("parameters").

Computational numerical exercises, presented in Sections 6 and 7, are intended to preliminarily validate the proposed correlated methods of "hole drilling" and "indentation". Section 8 contains closing remarks on this preliminary methodological study. Practical validations, related to real-life industrial situations and experiments, are subject of current research.

* Corresponding author. Tel.: +39 0223994221; fax: +39 0223994300.
E-mail address: giulio.maier@polimi.it (G. Maier).

2. Outline of the procedure for structural diagnosis by hole drilling test and indentation, combined in a sequence

The method presented with details in subsequent sections for estimation of both residual stresses and mechanical material properties is outlined here below as for the sequence of operative steps.

(I) The metallic workpiece to be investigated is preliminarily examined by an "expert" in the field, who provides the following basic information as "conjectures": location of the tests on the surface; a constitutive model for the material; "a priori" assumptions on the stress state to estimate, such as "uniformity" or "non-uniformity" along the hole depth; possibly principal axes directions if due to production process (e.g. lamination); selection of the parameters to identify (governing stress state and material model) and of conjectured lower and upper bound between which each unknown parameter will be sought; for each parameter to estimate a "reference value", which may coincide with the average of the conjectured lower and upper bound. In this preparatory stage, clearly, also possible standardizations and codes of practice are to be taken into account.

(II) The following experimental equipments are to be selected in the present method: hole drilling instrument [2]; instrumented indenter (e.g. [11]); digital image correlation (DIC) camera (see e.g. [12–14]). The HD features (depth, diame-ter, penetration steps) should be chosen within the set of standardized alternatives. The IND instrumentation apt to provide, in digitalized form, tip advancement versus force on the indenter can be selected among portable (no laboratory) equipments available on the market. As for DIC instrumentation, the specific operative requirement is the selection of the area around the hole and points on it where "full-field" (two- or three-dimensional) measurements of displacements will be performed (instead of strains measurements by "gauges rosette").

(III) Once-for-all for each category of HD + IND tests (primarily characterized by the chosen hole shape), the following usual computational operations are carried out: discretization mesh (here finite elements) exploiting possible symmetries; bound-ary and boundary conditions; selected computer code apt to large-strains simulations.

(IV) "Sensitivity analyses" are performed by test simulations ("direct analyses") using the results of the preceding stages. The following procedures, both starting from attribution of "reference values" (stage I) to all parameters, are often practically useful (primarily for selection of measurable quantities).
(α) Traditional sensitivity analysis, resting on partial derivatives approximated by finite differences (see e.g. [15]). Operatively, a perturbation (say $\pm 10\%$ of the interval between conjectured upper and lower bound) is generated in one (say p_i) of the sought parameters and consequences are computed, by test simulations, on representative measurable quantities u_j.
(β) Each representative "pseudo-experimental" quantity u_j is computed by attributing first, lower (say p_i') and, subsequently, upper bound (say p_i'') to parameter p_i while all the other parameters p_i are kept at their "reference values"; the difference between resulting values (say u_j' and u_j'') should be sufficiently larger than a homologous quantity representative of the measurement uncertainty.

(V) After the above preparatory stages (which may include suitable preliminary treatment of the surface), a HD test is performed as routinely. Displacements due to this test (or due to each step of it, if "stepwise" designed) are measured and digitalized by suitably located DIC instruments in pre-selected points (which may coincide with FE mesh nodes).

(VI) After removal of the HD instrument, an indentation (IND) is performed on the centre of the circular plane bottom surface of the hole by a conical indenter. The portable instrumented IND equipment provides, in digitalized form, "indentation curves", which numerically describe the penetration of the tip as a function of the force imposed on the indenter. Similar procedures are described for usual IND tests, e.g. in [11]. Additional to such IND experimental data, displacement measurements on the surface might be provided by DIC, again through digital photos before and after the indentation.

(VII) On the basis of the experimental data achieved by the two above outlined semi-destructive tests, inverse analyses are carried out, possibly "in situ", by means of pre-elaborated software, in order to achieve reliable estimates of the sought parameters. The resulting estimates quantify both the residual stress states and some meaningful mechanical properties of the material. There may be interactions between HD test and IND test: stresses to identify by the former might influence the latter and, vice versa, material parameters to identify by the latter (Young modulus primarily) influence the former.

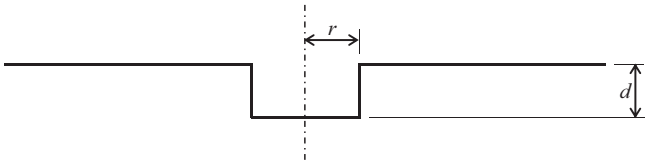

Fig. 1. Cylindrical shape of the hole generated by standardized HD tests.

Parameter estimations, also in view of the above interactions, are the subjects of Sections 5–7, after the preparatory procedures in next Sections 3 and 4 according to stages (III) and (IV) outlined in what precedes.

3. Mechanical modelling of both tests

3.1. Hole Drilling (HD) test

The problems tackled here in order to present and validate the proposed method are formulated numerically in what follows. To the drilled cylindrical hole the following data are attributed: depth $d = 2$ mm, radius $r = 2$ mm (Fig. 1). Residual stresses are assumed as two-dimensional in planes parallel to the surface of the tested structure, with reference axes x_1 and x_2 on the surface (supposed to be horizontal) and x_3 oriented inside.

The following stepwise-constant depth-dependence ("non-uniformity" in standard jargon) frequently assumed in practical applications of HD technique, is considered here for preliminary numerical checks of the proposed procedure:

$$\sigma_{11}(x_3) = \Sigma_1, \quad \sigma_{22}(x_3) = \Sigma_2, \quad \sigma_{12}(x_3) = \Sigma_3 \quad \text{along } 0 \le x_3 < \frac{d}{3} \tag{1a}$$

$$\sigma_{11}(x_3) = \Sigma_4, \quad \sigma_{22}(x_3) = \Sigma_5, \quad \sigma_{12}(x_3) = \Sigma_6 \quad \text{along } \frac{d}{3} \le x_3 < \frac{2d}{3} \tag{1b}$$

$$\sigma_{11}(x_3) = \Sigma_7, \quad \sigma_{22}(x_3) = \Sigma_8, \quad \sigma_{12}(x_3) = \Sigma_9 \quad \text{along } \frac{2d}{3} \le x_3 \le d \tag{1c}$$

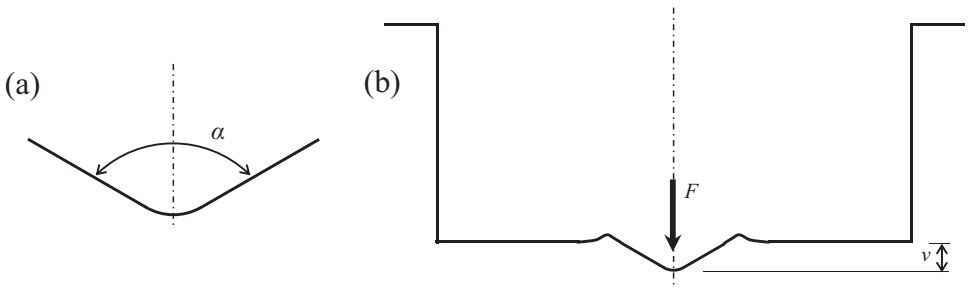

Fig. 2. Indentation (IND) after a HD test: (a) conical geometry of the indenter tip; (b) imprint with depth v generated by "load" F (schematic shape representation).

The stresses $\Sigma_1, \ldots, \Sigma_9$ are the parameters to identify. Accord-ing to stages (I) and (IV) of the procedure outlined in Section 2, conjectured "reference values" $\bar{\Sigma}_i$ (i = 1, . . ., 9) and "search intervals" $\Delta\bar{\Sigma}_i$ (centred on $\bar{\Sigma}_i$) are presented in Table 1(a), all in MPa.

3.2. Indentation (IND) test

On mechanical properties of the material, the following assumptions are considered in view of the indentation tests: homogeneity over the surrounding volume; isotropic elastoplasticity with isotropic hardening described by the classical Huber–Hencky–von Mises (HHM) model (e.g. [16]), namely in formulae:

$$\boldsymbol{\sigma} = \mathbf{D}\boldsymbol{\varepsilon}^e \tag{2}$$

$$\phi(\boldsymbol{\sigma}, \boldsymbol{\varepsilon}^p) = \sqrt{\frac{3}{2}\mathbf{S} : \mathbf{S}} - \bar{\sigma}(\boldsymbol{\varepsilon}_p) \le 0, \quad \boldsymbol{\varepsilon}_p = \sqrt{\frac{2}{3}\boldsymbol{\varepsilon}^p : \boldsymbol{\varepsilon}^p} \tag{3}$$

$$\bar{\sigma}(\boldsymbol{\varepsilon}_p) = \boldsymbol{\sigma}_Y^{1-H} E^H \left(\frac{\boldsymbol{\sigma}_Y}{E} + \boldsymbol{\varepsilon}_p\right)^H \tag{4}$$

$$\dot{\boldsymbol{\varepsilon}}^p = \frac{\partial\phi}{\partial\boldsymbol{\sigma}}\dot{\lambda}, \quad \dot{\lambda} \ge 0, \quad \phi\dot{\lambda} = 0 \tag{5}$$

In the above classical formulae: E and ν, in elasticity matrix $\mathbf{D}$, are the Young modulus and Poisson ratio, respectively, the lat-ter supposed to be "a priori" known (here ν = 0.3) in view of its marginal influence on structural safety margins; ϕ is the yield func-tion; $\bar{\sigma}$ represents the current yield stress, variable due to isotropic hardening according to Eq. (4) where σ_Y is the original value and H the hardening coefficient; $\boldsymbol{\sigma}$, $\mathbf{S}$, $\boldsymbol{\varepsilon}^e$ and $\boldsymbol{\varepsilon}^p$ are the tensors of stresses, deviatoric stresses, elastic and plastic strains, respectively; Eq. (5) expresses non-holonomy and associativity of metal plastic-ity, being $\dot{\lambda}$ the plastic multiplier rate.

Conjectured reference values and search intervals here attributed to the three sought parameters are specified in Table 1(b).

The indenter, assumed rigid in the present preliminary computational checks, exhibits conical shape (Fig. 2a) with circular cross section, angle α = 120° and spherically rounded tip with radius 0.2 mm. Coulomb friction is "a priori" assumed with coefficient f = 0.15.

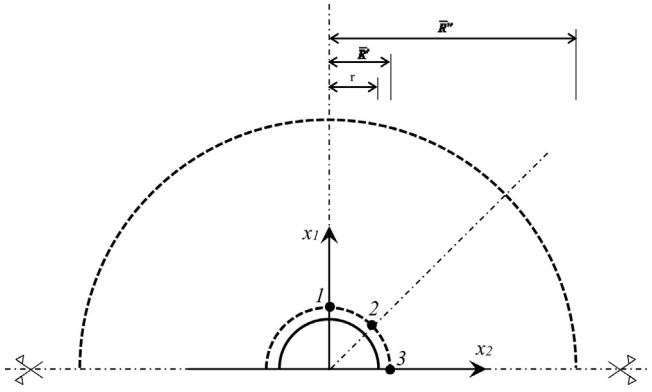

Fig. 3. The hole and two concentrical circles which define the area monitored by DIC on the structural component surface. Dots mark the material "nodes" whose displacements are employed in sensitivity analyses.

3.3. Domain around the hole

Fig. 3 shows the area where in plane displacements are here supposed to be measured by two-dimensional DIC: internal radius $\bar{R}' = 2.5$ mm; external radius $\bar{R}'' = 10.0$ mm.

The finite elements (FE) three-dimensional discretization adopted to the present purposes for modelling both HD and IND exhibits the following features (Fig. 4): axial symmetry with respect to the central vertical axis x_3; cylindrical domain with radius R = 20 mm and depth D = 6 mm for FE simulations; boundary conditions assumed as zero displacements on the lateral cylindrical and bottom surface where "perturbations" due to both tests are supposed to be negligible; zero loads on internal hole surface after drilling and on the surface of the tested structural component; displacement field discretization by FE with mesh visualized in Fig. 4 and including 32269 elements; the degrees-of-freedom num-ber amounts to 109104; the code employed is the commercial FE

Table 1
"Reference values" and "conjectured intervals" of the parameters to identify: (a) residual stresses $\bar{\Sigma}_i$, i = 1, . . ., 9 [MPa]; (b) parameters in elastic–plastic HHM model.

(a)

	1st layer			2nd layer			3rd layer		
$\bar{\Sigma}_i$	220	−220	65	100	−100	25	50	−50	15
$\Delta\bar{\Sigma}_i$	80	80	30	50	50	30	30	30	30

(b)

$\bar{E}$	$\bar{\sigma}_Y$	$\bar{H}$	$\Delta\bar{E}$	$\Delta\bar{\sigma}_Y$	$\Delta\bar{H}$
190000 MPa	600 MPa	0.08	40000 MPa	300 MPa	0.16

Table 2
Some representative sensitivities of measurable displacements generated by the HD test, in the presence of "non-uniform" residual stresses at their conjectured "reference values" $\bar{\Sigma}_i$ gathered in Table 1(a).

	$\bar{u}_1 = 2.78$ μm		$\bar{u}_2 = 1.44$ μm		$\bar{u}_3 = 2.78$ μm	
	δu_1	S_{i1}	δu_2	S_{i2}	δu_3	S_{i3}
Σ_1	3.03%	0.67	2.49%	0.55	0.53%	0.12
Σ_4	1.15%	0.12	1.09%	0.11	0.44%	0.04
Σ_7	0.55%	0.03	0.53%	0.03	0.30%	0.02
E	−2.06%	−0.98	−2.06%	−0.98	−2.06%	−0.98

code Abaqus, accounting for large-strains structural responses as expected in the IND phases of the present applications [17].

4. Test simulations and sensitivity analyses

Modelling assumptions and numerical data gathered in the preceding Section 3 here below are employed for "direct analyses" as orientative preliminaries to the "inverse analyses" dealt with in Sections 5–7.

4.1. On HD tests

According to the present hypothesis of stepwise-constant non-uniformity of residual stresses, Eq. (1), nine parameters Σ_i (with i = 1, . . ., 9) are to identify. The "reference values" $\bar{\Sigma}_i$ in Table 1(a) are attributed to the sought parameters and, subsequently, these values are increased by $\delta\Sigma_i$ = 10 MPa as a perturbation performed on each parameter, separately in a sequel. With such 9 different inputs in terms of stress parameters, the consequent simulations are carried out by the FE model formulated in Section 3.

The "pseudo-experimental" value u_j resulting from each computation, if compared to that computed before perturbation, leads to a quantification of the consequence on measurements (namely δu_j) due to the above specified perturbation. Clearly, the change in pseudo-experimental measurement divided by the parameter change causing it provides the usual "sensitivity" S_{ij} as finite difference approximation of the partial derivative [15], namely:

$$\frac{\delta u_j}{\delta \bar{\Sigma}_i} \cong \frac{\partial u_j}{\partial \bar{\Sigma}_i} = S_{ij} \tag{6}$$

In order to check the identifiability of residual stress parameters by the HD tests specified in Section 3, some representative "sensi-tivities" among those formulated above are gathered in Table 2 as follows.

The first column indicates the three (among the 9 listed in Table 1) parameters changed by a perturbation while all the other eight stresses remain at the reference values $\bar{\Sigma}_i$.

The row shows (in μm) the measurable modulus $\bar{u}_j$ of each displacement vector computed by test simulation in points j = 1, 2, 3 (see Fig. 3) before the above specified perturbations of $\delta\Sigma_i$ = +10 MPa on stress parameters $\bar{\Sigma}$. The consequences of such perturbation on each Σ_i (i = 1, 4, 7) and on Young modulus E as well, are gathered as percentage in the first column, while the second one contains the sensitivities according to Eq. (6). Similar numerical results concerning two other representative DIC pseudo-
experimental data (u_2, u_3) are collected in the other two columns pairs.

It is meaningful to underline here the following limitations (to be re-considered later) of the above "direct analyses": linear elasticity with known moduli has been assumed; plastic strains due to stress changes caused by drilling were ruled out "a priori".

4.2. On IND test

Now the IND test is considered with the input specified in Section 3 and, preliminarily, with the hypothesis that residual stresses can be disregarded, since they are substantially reduced by the preceding HD test.

The IND test is simulated by means of the same FE model employed for HD and now by means of the HHM elastoplastic model, Eqs. (2)–(5), calibrated with the "reference values" specified in Section 3.2. The resulting "pseudo-experimental" data are gathered in Table 3 and the relevant indentation curves are shown in Fig. 5.

The difference between up and down curve in Fig. 5 obviously is caused by the plastic strains involved by the generated imprint. On friction a Coulomb model is assumed with non-associativity (no dilatancy) and with parameter f = 0.15 (which might be considered in practical applications as a parameter to identify, additional to those in the elastic–plastic model).

Table 4 gathers numerical results similar to those in Table 2, but now concerning sensitivity of representative experimental data from IND tests, namely: maximal penetration V. In Table 4, top row, $\bar{V}$ represents the value achieved by test simulations. Each row

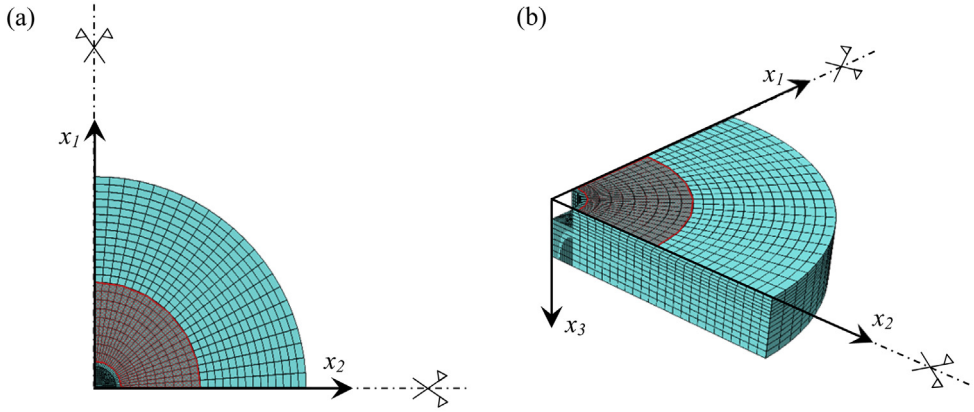

Fig. 4. Domain and mesh for FE simulations of both HD and IND tests; the DIC monitored area is highlighted.

Table 3
Numerical "pseudo-experimental" data visualized in indentation curves of Fig. 5: v' entering; v'' exit.

F [N]	0	100	200	300	400	500	600	700	800	900	1000
v' [μm]	0	39	67	88	107	124	141	157	173	192	211
v'' [μm]	201	204	206	207	207	208	208	209	209	210	211

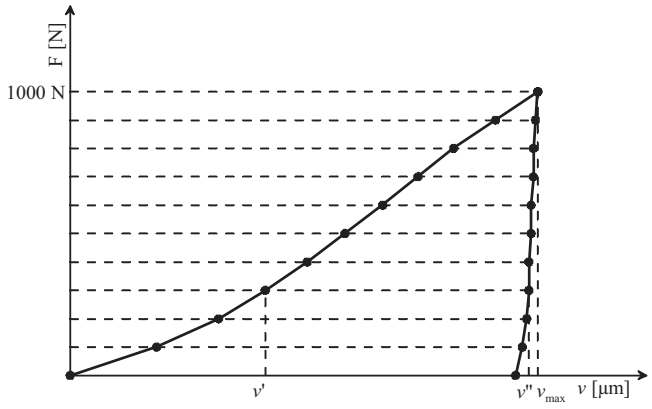

Fig. 5. Results of IND test simulation: penetration v versus loading force F on the indenter (v' entering, v'' exit).

Table 4
Sensitivities of indenter penetration V by the IND test after HD test, in the absence of residual stresses.

	$\bar{V} = 211.1$ μm (211.9 μm)	
	ΔV	S_{iV}
E	−2.9	−0.156
σ_Y	−10.4	−0.175
H	−3.8	−484.7

concerns sensitivities with respect to the HHM parameter specified in the first column.

The IND test has been simulated also by inserting in the FE model the residual stresses resulting from the preceding HD test. The following numerical results have been achieved: V = 211.9 μm, u_1 = 0.085 μm, u_2 = 0.029 μm, u_3 = 0.081 μm; with-out such "re-residual stresses": $\bar{V}$= 211.1 μm, $\bar{u}_1 = 0.086$ μm, $\bar{u}_2 = 0.029$ μm, $\bar{u}_3$ = 0.082 μm. Comparisons of the correspond-ing above results evidence the acceptability of the hypothesis that there are no more residual stresses when the IND test is performed after the HD test. Such expected lack of sensitivity in practice evi-dences that DIC measurements are superfluous in the IND stage of present HD + IND method.

5. Inverse analysis procedures based on both hole drilling and indentation tests

"Direct analysis" (namely tests simulation) provides the relationship $\mathbf{u}(\mathbf{p})$ between the vector of sought parameters $\mathbf{p}$ and the vector $\mathbf{u}$ of measurable quantities. Experimental or, like here, "pseudo-experimental" data $\bar{\mathbf{u}}$ represent the input for inverse analysis, which here and in a vast literature (e.g. [18–21]) is formulated as follows:

$$\omega_{\min} = \min_{\mathbf{p}} \omega(\mathbf{p}), \quad \mathbf{p} \in \Omega \tag{7a}$$

$$\omega(\mathbf{p}) = [\bar{\mathbf{u}} - \mathbf{u}(\mathbf{p})]^T \mathbf{C}^{-1} [\bar{\mathbf{u}} - \mathbf{u}(\mathbf{p})] \tag{7b}$$

Matrix $\mathbf{C}$ is the "covariance matrix" which quantifies the inaccuracies of the experimental data and through its inversion implies more role to more accurate measurements. In this preliminary study, without real-life tests, $\mathbf{C}$ is assumed as identity matrix and the deterministic approach is adopted leading to the "estimates" vector $\bar{\bar{\mathbf{p}}}$ as solution of problem (7). The "search domain" Ω is based on conjectures by "experts" as pointed out in Section 3.

To the present purposes the optimization problem Eq. (7) exhibit two kinds of mathematical features, depending on the linearity or nonlinearity of function $\mathbf{u}(\mathbf{p})$ as discussed in what follows.

(I) Linear elasticity can be reasonably attributed in present HD practice to the relationship which connects the residual stresses to their consequences in terms of measurable deformations $\mathbf{u}$ due to drilling generating the hole. Inelastic strains are supposed not to occur if residual stresses do not exceed 80% of the yield stress, as for "thick" structural components [2]. According to the hypothesis of stepwise-constant dependence of residual stresses on depth x_3, Eq. (1), linear is the dependence of measurable deformations on the parameters to identify (Section 3). Therefore, function $\mathbf{u}(\mathbf{p})$ in Eq.(7), $\mathbf{p}$ being now vector $\{\Sigma_1, \ldots, \Sigma_9\}^T$, can be formulated as:

$$\mathbf{u} = \mathbf{M}\mathbf{p} \tag{8}$$

where matrix $\mathbf{M}$ can be computed once-for-all on the basis of (known or conjectured) elastic moduli (E and ν).

If the linear relation Eq. (8) holds, the solution $\bar{\bar{\mathbf{p}}}$ of optimization problem (7) turns out to be achievable economically in the following "closed-form":

$$\bar{\bar{\mathbf{p}}} = \mathbf{V}\mathbf{M}^T\bar{\mathbf{u}}, \quad \text{where} \quad \mathbf{V} = (\mathbf{M}^T\mathbf{M})^{-1} \tag{9}$$

(II) Since inelastic strains are produced by IND tests, the link between sought parameters $\mathbf{p}$ and related measurable quanti-ties $\mathbf{u}$ is nonlinear. For the calibration of elastic–plastic material models, like the classical one described by Eqs. (2)–(5), the discrepancy minimization for parameters estimation, problem (7), might exhibit lack of convexity in the objective functions and ill-posedness in the formulation, particularly if choice and number of experimental data are inadequate. For numerical applications in practice the following methodologies provide at present algorithms implemented in commercial codes: nonlinear mathematical pro-gramming by Trust Region Algorithms (TRA); Genetic Algorithms; Artificial Neural Networks.

The TRA implemented in code Matlab is adopted in this study and outlined here below in 3 stages, without details or computational comparisons with possible alternatives in view of the vast literature now available, e.g. [22,23].

(i) An initialization is performed by selecting an initial vector $\mathbf{p}_0$ of parameters within the "search domain" conjectured by an expert. At each step starting from $\mathbf{p}_j$ first-order derivatives of the function $\omega(\mathbf{p})$, Eq. (7b), are computed at $\mathbf{p}_j$ by (here forward) finite-difference and are employed for the approximation at $\mathbf{p}_j$ of the Hessian matrix of $\omega(\mathbf{p})$ by means of its gradient and its Jacobian matrix. Thus, the objective function (7b) is approximated as a quadratic function of the increments $\Delta\mathbf{p}_j$ as variables, with linearity in increments only and under inequality constraints included in the material model.

(ii) The approximated minimization problem formulated at stage (i) turns out to be a quadratic programming problem in the increments $\Delta\mathbf{p}_j$ as constrained variables, to be solved by a traditional algorithm of nonlinear programming implemented in the TRA software [24]. The resulting solution $\bar{\Delta\mathbf{p}}_j$ quantifies the

step and the point $\mathbf{p}_{j+1} = \mathbf{p}_j + \Delta\bar{\mathbf{p}}_j$; starting from this point the two above stages are performed again as subsequent step.

(iii) At the end of each step the objective function is assessed as different from zero by a quantity compatible with computational and algorithmic approximations. If these checks are not reliable another initialization is selected and the above procedure is repeated, also in order to possibly avoid convergence of the step sequence to a local minimum instead to the absolute minimum.

6. Computational procedures for structural diagnosis by correlated HD and IND tests

The experimental data provided by HD + IND tests can be exploited for estimation of both stresses and elastic–plastic properties according to the procedure outlined in what follows.

(A) Inverse analysis is performed based on the experimental data from IND test (indentation curve only, no DIC measurements in view of sensitivity analyses in Section 4), by assuming that there are no residual stresses (assumption motivated by other sensitivity analysis in Section 4).

(B) The material parameters estimates generated by the preceding (A) inverse analysis, (Young modulus E alone in the present validation exercise) are input into the FE model adopted for simulations of HD tests. Such simulations consist of modelling the consequences, in terms of DIC measurable displacements, of stresses governed by parameters Σ as loads on the hole cylindrical surface. Solution of discrepancy function minimization consists now of stresses opposite in sign to the residual stresses existing there before the drilling operation. Matrix $\mathbf{M}$ in Eq. (8) is generated and estimates (here $\{\bar{\bar{\Sigma}}_1, \ldots, \bar{\bar{\Sigma}}_9\}^T = \bar{\bar{\mathbf{p}}}$) of the parameters governing stresses (here through Eq. (1)) are achieved according to Eq. (9). If Young modulus alone is transferred from the IND stage, matrix $\mathbf{M}$ may be merely scaled with respect to the reference value.

The interactions between HD stage and IND stage might be in diverse applications not as weak as exhibited by the present example. In view of such prospect the following further computational steps are proposed here and numerically performed in Section 7.

(C) The stress parameters identified in the above stage (B) govern a stress field over the whole domain (with zero stress on the hole surface) which is now inserted into the FE model. The inverse analysis concerning the results from test IND is carried out again as stage (C).

(D) After same transition like the one from (A) to (B). by using updated modulus E in matrix $\mathbf{M}$, inverse analysis based on the same test HD results is carried out.

It is reasonably expected that the above iterative sequence converges rapidly to estimates of the sought parameters, both of stress state and elastoplasticity.

7. Computational example of the HD + IND inverse analysis procedure

The first numerical exercise for validation of the proposed diagnostic procedure concerns the estimation of parameters E, σ_Y, H in HHM model, Eqs. (2)–(5), by backanalysis based as input on the pseudo-experimental measurements ("direct analysis") by instrumented indenter. These data are computed through IND test simulation by FEM as described in Sections 3 and 4. By neglecting any possible "re-residual stresses" after the preceding HD test, the algorithm TRA is applied twice with two different initializations.

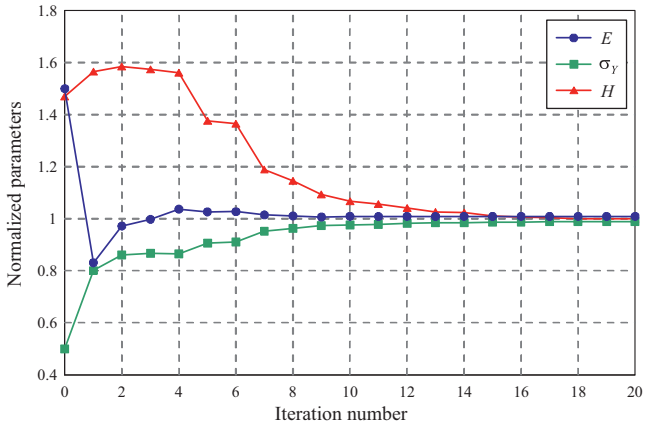

Fig. 6. Step sequence of a TRA application to backanalysis of IND test.

One TRA step sequence is visualized in Fig. 6; it implied 20 steps with an end criterion of 10^{-5} for variation of discrepancy function or 0.002 for variations of normalized parameters. The computing time turned out to be 160 min by a computer with the following features: Intel® Core™ i7-2600 CPU @ 3.4 GHz, with 16 GB of RAM.

With same criterion but different initialization (namely $E = 95000$ MPa, $\sigma_Y = 300$ MPa, $H = 0.08$) steps turned out to be 14 and computing time 120 min.

A check of computational accuracy can be derived by comparing the estimates provided by the backanalysis to the parameters values employed as input of the test simulation leading to the pseudo-experimental data: such differences turn out to be less than 1%.

The number of displacement components measurable by DIC (two-dimensional) in nodes of preselected grid around the hole (Fig. 4) amounts to 1760. Clearly, at growing distance from the hole axis, displacements due to drilling decreases. Therefore, the num-ber of DIC measurements to be employed for backanalysis can be reduced with decrease of matrix $\mathbf{M}$ size. However, such decrease does not influence the computing time in the present inverse anal-ysis procedure. The Young modulus estimate E = 191710 MPa is now fed into the formulation of the 1760 × 9 matrix $\mathbf{M}$, Eq. (9), and hence of matrix $\mathbf{V}$ of order 9, Eq. (9), linearly leading to the estimates (vector $\bar{\bar{\Sigma}}_1$) of the 9 parameters $\bar{\bar{\Sigma}}$governing the sought residual stress state.

Matrix $\mathbf{V}$ is generated (computing time 9 minutes) once-for-all for any estimation of residual stresses interpreted as plane states uniform in each of three pre-selected layers (Section 3).

The estimates $\bar{\bar{\Sigma}}_i (i = 1, \ldots, 9)$ provided by Eq. (9) in the present example are gathered in Table 5 and turn out to almost coincide with the "reference values" of Table 1, namely with the values assumed as the actual "exact" once for the generation (in Section 3) of the "pseudo-experimental" input for the HD inverse analysis. As expected, from the sensitivity analyses in Section 4, stages (C) and (D) turn out to be redundant here and also in most rou-tine practical applications of this diagnostic procedure on structural components of frequent kind as for materials and service.

8. Closing remarks

The research results presented in what precedes lead to the following conclusions.

(i) The "quasi-non-destructive" hole drilling (HD) and indentation (IND) experiments can be combined and carried out in the same location for structural diagnosis of metallic components. Such novel procedure obviously gives rise to much less

Table 5
Backanalysis estimates of the parameters governing the residual stress model [MPa].

1st layer			2nd layer			3rd layer		
$\bar{\bar{\Sigma}}_1$	$\bar{\bar{\Sigma}}_2$	$\bar{\bar{\Sigma}}_3$	$\bar{\bar{\Sigma}}_4$	$\bar{\bar{\Sigma}}_5$	$\bar{\bar{\Sigma}}_6$	$\bar{\bar{\Sigma}}_7$	$\bar{\bar{\Sigma}}_8$	$\bar{\bar{\Sigma}}_9$
222	−222	66	101	−101	25	51	−50	15

"damages" than those frequently generated by HD test for residual stress estimation and separately by "small punch" tests for material models calibration, both standardized separately at present.

(ii) Parameters which govern residual stresses and elastic–plastic material behaviour can be identified by fast non-stochastic inverse analyses based on experimental data provided by a HD test first and by IND test second, with a common FE model and with fast convergence as for the interactions between the two estimations of parameters. As intuitively expected in most practical applications and here corroborated by computational exercises, the influences on IND of residual stresses after HD are negligible. Therefore, inverse analysis on IND measurements is done first and provides the estimated Young modulus necessary for the inverse analysis based on the HD test with stress parameters only as unknowns to identify.

(iii) The whole diagnostic procedure can be carried out "in situ" (no laboratory) in a fast and economical fashion by portable instruments, namely: drilling device, instrumented indenter, digital image correlation cameras (instead of traditional strain gauges), small computer with pre-elaborated software.

The above results are here only computationally corroborated by preliminary examples with some simplifications and specializations, such as the assumption (frequent in present practice) of piece-wise constant variation along the hole depth of the residual stresses to estimate.

Extensions to more general stress and material models, to possible inelastic deformations in HD tests, and to stochastic approaches are desirable developments and current research purposes.

A remarkable limitation of the present study arises from the geometry of the hole with diameter larger than depth. Such feature, necessary for indentation on the hole bottom surface, is frequently adopted in present practice of metallic components diagnosis. For different hole geometries, a diverse HD + IND technique with indentation at the hole edge on the surface is a subject of current investigation.

Acknowledgements

The authors are grateful to the Engineers of RTM Breda for useful information on HD test equipment in their Cormano laboratory.

References

[1] A. Ajovalasit, M. Scafidi, B. Zuccarello, M. Beghini, L. Bertini, C. Santus, E. Valentini, A. Benincasa, L. Bertelli, The Hole Drilling Strain Gauge Method for the Measurement of Uniform or Non-uniform Residual Stresses (AIAS–TR01:2010), AIAS, Florence, 2010.
[2] ASTM, Standard Test Method for Determining Residual Stresses by Hole-Drilling Strain-Gage Method (E837-13a), ASTM International, West Conshohocken, PA, 2013.
[3] X. Huang, Z. Liu, H. Xie, Recent progress in residual stress measurement techniques, Acta Mech. Solida Sin. 26 (2013) 570–583.
[4] G.S. Schajer (Ed.), Practical Residual Stress Measurement Methods, Wiley, Chichester, 2013.
[5] G.S. Schajer, Measurement of non-uniform residual stresses using the hole-drilling method. Part I. Stress calculation procedures, Trans. ASME 110 (1988) 338–343.
[6] P.J. Withers, H.K.D.H. Bhadeshia, Residual stresses. Part 1. Measurement techniques, Mater. Sci. Technol. 17 (2001) 355–365.
[7] M.R. VanLandingham, Review of instrumented indentation, J. Res. Natl. Inst. Stand. Technol. 108 (2003) 249–265.
[8] M. Bocciarelli, G. Maier, Indentation and imprint mapping method for identification of residual stresses, Comput. Mater. Sci. 39 (2007) 381–392.
[9] G. Bolzon, V. Buljak, An indentation-based technique to determine in-depth residual stress profiles induced by surface treatment of metal components, Fatigue Fract. Eng. Mater. Struct. 34 (2010) 97–107.
[10] V. Buljak, G. Maier, Identification of residual stresses by instrumented elliptical indentation and inverse analysis, Mech. Res. Commun. 41 (2012) 21–29.
[11] V. Buljak, G. Maier, Proper orthogonal decomposition and radial basis functions in material characterization based on instrumented indentation, Eng. Struct. 33 (2011) 492–501.
[12] A. Baldi, Residual stress measurement using hole drilling and integrated digital image correlation techniques, Exp. Mech. 54 (2014) 379–391.
[13] J.D. Lord, D. Penn, P. Whitehead, The application of digital image correlation for measuring residual stress by incremental hole drilling, Appl. Mech. Mater. 13–14 (2008) 65–73.
[14] D.V. Nelson, A. Makino, T. Schmidt, Residual stress determination using hole drilling and 3D image correlation, Exp. Mech. 46 (2006) 31–38.
[15] M. Kleiber, H. Antúnez, T.D. Hien, P. Kowalczyk, Parameter Sensitivity in Nonlinear Mechanics, Wiley, Chichester, 1997.
[16] Z.P. Bažant, M. Jirásek, Inelastic Analysis of Structures, Wiley, Chichester, 2002.
[17] Abaqus/Standard, Theory and User's Manuals – Release 6.13, Dassault Systèmes Simulia Corp., Providence, RI, 2013.
[18] H.D. Bui, Inverse Problems in the Mechanics of Materials: An Introduction, CRC Press, Boca Raton, 1994.
[19] G. Maier, V. Buljak, T. Garbowski, G. Cocchetti, G. Novati, Mechanical characterization of materials and diagnosis of structures by inverse analyses: some innovative procedures and applications, Int. J. Comput. Methods 11 (2014) 1–25.
[20] Z. Mróz, G.E. Stavroulakis (Eds.), Parameter Identification of Materials and Structures, Springer, New York, 2005.
[21] A. Tarantola, Inverse Problem Theory and Methods for Model Parameter Estimation, Society for Industrial and Applied Mathematics, Philadelphia, 2005.
[22] A.R. Conn, N.I.M. Gould, P.L. Toint, Trust-Region Methods, Society for Industrial and Applied Mathematics, Philadelphia, 2000.
[23] J. Nocedal, S.J. Wright, Numerical Optimization, 2nd ed., Springer, New York, 2006.
[24] Matlab, Matlab User's Guide – Release 2014a, The MathWorks Inc., Natick, MA, 2014.